
An ultra-weak finite element method
for the pressure Poisson equation

D. R. Q. Pacheco, O. Steinbach

**Berichte aus dem
Institut für Angewandte Mathematik**

Technische Universität Graz

An ultra-weak finite element method
for the pressure Poisson equation

D. R. Q. Pacheco, O. Steinbach

**Berichte aus dem
Institut für Angewandte Mathematik**

Bericht 2021/17

Technische Universität Graz
Institut für Angewandte Mathematik
Steyrergasse 30
A 8010 Graz

WWW: <http://www.applied.math.tugraz.at>

© Alle Rechte vorbehalten. Nachdruck nur mit Genehmigung des Autors.

An ultra-weak finite element method for the pressure Poisson equation

Douglas R. Q. Pacheco, Olaf Steinbach

Institut für Angewandte Mathematik, TU Graz,
Steyrergasse 30, 8010 Graz, Austria

Abstract

A Poisson equation can be derived from the Stokes or Navier–Stokes system to write the pressure p in terms of the velocity \mathbf{u} . For this inverse problem to determine $p \in L^2(\Omega)$, we propose and analyze an ultra-weak variational formulation in which integration by parts is applied to shift all derivatives to the test functions. This allows using discontinuous trial spaces and also to consider less regular data. The unique solvability of the resulting Galerkin–Petrov formulation is based on an inf–sup stability condition, and optimal convergence is proven on the discrete level for compatible spaces. We also propose a conforming finite element method using piecewise constant trial functions and appropriate second–order test spaces, both for tensor–product meshes using second–order B–splines, and for unstructured simplicial meshes using lowest–order Raviart–Thomas elements. Numerical experiments confirm the a priori error estimates, revealing optimal convergence for uniform and adaptive meshes.

1 Introduction

In fluid flow systems, using the velocity field to compute the pressure is a task with established relevance in both theory and engineering practice. For example, this can be used in fractional–step solvers to update the pressure from a previously computed velocity [6], or in clinical practice to estimate arterial pressure from imaging–based velocity measurements [7]. The most popular approach to solve this inverse problem is the so-called pressure Poisson equation (PPE) obtained from the divergence of the Navier–Stokes momentum equation. Of course, applying the divergence increases the regularity requirements on the unknown pressure p and the given velocity \mathbf{u} , imposing challenges to both the analysis and the discretization via finite elements. In fact, standard (weak) variational formulations for the PPE require continuous pressure and smooth velocities for conformity, which is sometimes circumvented through projections [10]. In this context, we introduce here an ultra-weak variational formulation for the PPE and a conforming finite element method

for its discretization. The first and perhaps only time an ultra-weak formulation has been mentioned – yet not analysed nor discretized – for the PPE was in an article by Sani et al. [11] on pressure boundary conditions. Apart from that, ultra-weak formulations are normally either given for barely first-order boundary value problems [4] (where standard Lagrangian finite element spaces can be used), or handled as a mixed problem so as to circumvent smoothness requirements on the test space [2]. Our idea, on the other hand, is to work with more regular test functions, which allows us to stay with a standard L^2 requirement for the pressure.

As a model problem, we consider the Dirichlet boundary value problem for the Stokes system,

$$-\Delta \mathbf{u} + \nabla p = \mathbf{f}, \quad \operatorname{div} \mathbf{u} = 0 \quad \text{in } \Omega, \quad \mathbf{u} = \mathbf{0} \quad \text{on } \Gamma, \quad (1.1)$$

where $\Omega \subset \mathbb{R}^n$, $n = 2, 3$, is a bounded domain with Lipschitz boundary $\Gamma = \partial\Omega$, and \mathbf{f} is given. The standard variational formulation of (1.1) is to find $(\mathbf{u}, p) \in \mathbf{H}_0^1(\Omega) \times L_0^2(\Omega)$ such that

$$\sum_{i=1}^n \int_{\Omega} \nabla u_i \cdot \nabla v_i \, dx + \int_{\Omega} \nabla p \cdot \mathbf{v} \, dx = \int_{\Omega} \mathbf{f} \cdot \mathbf{v} \, dx, \quad \int_{\Omega} \operatorname{div} \mathbf{u} \, q \, dx = 0 \quad (1.2)$$

is satisfied for all $(\mathbf{v}, q) \in \mathbf{H}_0^1(\Omega) \times L_0^2(\Omega)$. Note that the pressure p is only unique up to an additive constant, hence we use the scaling condition $p \in L_0^2(\Omega)$, i.e., $p \in L^2(\Omega)$ satisfying

$$\int_{\Omega} p(x) \, dx = 0. \quad (1.3)$$

A stable finite element discretization of the variational formulation (1.2) requires the use of inf-sup stable finite elements $(\mathbf{v}_h, q_h) \in \mathbf{V}_h \times X_h \subset \mathbf{H}_0^1(\Omega) \times L_0^2(\Omega)$, e.g., the lowest-order Taylor-Hood pair using continuous second-order approximations for the velocity \mathbf{u} , and continuous piecewise linear approximations for the pressure p . It is well known that the lowest-order \mathbf{P}_1/P_0 approximation using piecewise linears and piecewise constants for the velocity and for the pressure, respectively, results in an unstable discretization. In this case one may consider stabilization techniques to obtain stable discretization schemes for (1.2). This stabilization can be based on the pressure Poisson equation obtained formally when considering the divergence of the momentum equation in (1.1). This results in a Poisson equation for the pressure p which is still considered in $L_0^2(\Omega)$, and hence requires the use of an ultra-weak variational formulation.

2 The pressure Poisson equation

In the strong formulation, the pressure Poisson equation can be obtained by applying the divergence to the momentum equation in (1.1):

$$-\Delta p = -\operatorname{div}(\Delta \mathbf{u} + \mathbf{f}) =: -\operatorname{div} \tilde{\mathbf{f}} \quad \text{in } \Omega, \quad \int_{\Omega} p \, dx = 0. \quad (2.1)$$

It is obvious that this does not define a unique p , since any harmonic function with vanishing mean can be added. Hence we consider the Neumann boundary condition

$$\frac{\partial}{\partial n_x} p = (\mathbf{f} + \Delta \mathbf{u}) \cdot \mathbf{n}_x \quad \text{on } \Gamma, \quad (2.2)$$

which is obtained from the balance of momentum in the normal direction along Γ . To include the Neumann boundary condition into the variational formulation, we multiply the pressure Poisson equation (2.1) with a sufficiently regular test function φ and integrate over Ω ,

$$\int_{\Omega} [-\Delta p] \varphi \, dx = - \int_{\Omega} \operatorname{div} \tilde{\mathbf{f}} \varphi \, dx.$$

Doing integration by parts on both sides, this gives

$$\int_{\Omega} \nabla p \cdot \nabla \varphi \, dx - \int_{\Gamma} \frac{\partial}{\partial n_x} p \varphi \, ds_x = \int_{\Omega} \tilde{\mathbf{f}} \cdot \nabla \varphi \, dx - \int_{\Gamma} \tilde{\mathbf{f}} \cdot \mathbf{n}_x \varphi \, ds_x,$$

and inserting the Neumann boundary condition (2.2) we obtain

$$\int_{\Omega} \nabla p \cdot \nabla \varphi \, dx - \int_{\Gamma} [(\mathbf{f} + \Delta \mathbf{u}) \cdot \mathbf{n}_x] \varphi \, ds_x = \int_{\Omega} \tilde{\mathbf{f}} \cdot \nabla \varphi \, dx - \int_{\Gamma} \tilde{\mathbf{f}} \cdot \mathbf{n}_x \varphi \, ds_x,$$

i.e.,

$$\int_{\Omega} \nabla p \cdot \nabla \varphi \, dx = \int_{\Omega} \tilde{\mathbf{f}} \cdot \nabla \varphi \, dx.$$

Now, applying integration by parts once again on the left-hand side results in

$$\int_{\Gamma} p \frac{\partial}{\partial n_x} \varphi \, ds_x + \int_{\Omega} p [-\Delta \varphi] \, dx = \int_{\Omega} \tilde{\mathbf{f}} \cdot \nabla \varphi \, dx,$$

and requesting $\partial_n \varphi = 0$ on Γ yields

$$\int_{\Omega} p [-\Delta \varphi] \, dx = \int_{\Omega} \tilde{\mathbf{f}} \cdot \nabla \varphi \, dx.$$

Finally, we include the zero mean pressure condition and obtain an extended variational formulation to find $p \in X := L^2(\Omega)$ such that

$$\int_{\Omega} p [-\Delta \varphi] \, dx + \frac{1}{|\Omega|} \int_{\Omega} p \, dx \int_{\Omega} \varphi \, dx = \int_{\Omega} \tilde{\mathbf{f}} \cdot \nabla \varphi \, dx \quad (2.3)$$

for all $\varphi \in Y := \{\varphi \in H_{\Delta}^1(\Omega) : \partial_n \varphi = 0 \text{ on } \Gamma\}$, where

$$H_{\Delta}^1(\Omega) := \left\{ \varphi \in H^1(\Omega) : \Delta \varphi \in L^2(\Omega) \right\},$$

and

$$|\Omega| := \int_{\Omega} dx.$$

Unique solvability of the ultra-weak variational formulation (2.3) is based on an inf-sup stability condition for the bilinear form

$$a(p, \varphi) := \int_{\Omega} p [-\Delta \varphi] dx + \frac{1}{|\Omega|} \int_{\Omega} p dx \int_{\Omega} \varphi dx, \quad p \in X, \varphi \in Y.$$

While the norm for $p \in X = L^2(\Omega)$ is obvious, for $\varphi \in H^1(\Omega)$ an equivalent norm is given by

$$\|\varphi\|_{H^1(\Omega), \Omega}^2 := \|\nabla \varphi\|_{L^2(\Omega)}^2 + \frac{1}{|\Omega|} \left(\int_{\Omega} \varphi(x) dx \right)^2.$$

For $\varphi \in H_{\Delta}^1(\Omega)$ we therefore define the norm

$$\|\varphi\|_{H_{\Delta}^1(\Omega)}^2 := \|\nabla \varphi\|_{L^2(\Omega)}^2 + \frac{1}{|\Omega|} \left(\int_{\Omega} \varphi(x) dx \right)^2 + \|\Delta \varphi\|_{L^2(\Omega)}^2.$$

At this time we recall Poincaré's inequality, i.e., for all $u \in H^1(\Omega)$ we have

$$\int_{\Omega} [u(x) - u_{\Omega}]^2 dx \leq c_P \int_{\Omega} |\nabla u(x)|^2 dx, \quad u_{\Omega} = \frac{1}{|\Omega|} \int_{\Omega} u(x) dx, \quad (2.4)$$

which is equivalent to

$$\int_{\Omega} [u(x)]^2 dx \leq \frac{1}{|\Omega|} \left(\int_{\Omega} u(x) dx \right)^2 + c_P \int_{\Omega} |\nabla u(x)|^2 dx. \quad (2.5)$$

Now we are in a position to state an equivalent norm in $Y \subset H_{\Delta}^1(\Omega)$, i.e.,

$$\|\varphi\|_Y^2 := \|\Delta \varphi\|_{L^2(\Omega)}^2 + \frac{1}{|\Omega|} \left(\int_{\Omega} \varphi(x) dx \right)^2.$$

Lemma 2.1 *For $\varphi \in Y \subset H_{\Delta}^1(\Omega)$ there hold the norm equivalence inequalities*

$$c_{\text{equiv}} \|\varphi\|_{H_{\Delta}^1(\Omega)}^2 \leq \|\varphi\|_Y^2 \leq \|\varphi\|_{H_{\Delta}^1(\Omega)}^2, \quad c_{\text{equiv}} := \frac{1}{\max\{1 + c_P, 1 + c_P^{-1}\}}.$$

Proof. While the upper estimate is trivial, it remains to prove the lower bound. For $\varphi \in Y$ we have, when applying Green's first formula and using $\partial_n \varphi = 0$ on Γ ,

$$\begin{aligned} \|\nabla \varphi\|_{L^2(\Omega)}^2 &= \int_{\Omega} \nabla \varphi \cdot \nabla \varphi dx = \int_{\Gamma} \partial_n \varphi \varphi ds_x + \int_{\Omega} [-\Delta \varphi] \varphi dx \\ &= \int_{\Omega} [-\Delta \varphi] \varphi dx \leq \|\Delta \varphi\|_{L^2(\Omega)} \|\varphi\|_{L^2(\Omega)}. \end{aligned}$$

Now, using Young's inequality for some $\varepsilon > 0$ and the Poincaré inequality (2.5), this gives

$$\begin{aligned} \|\nabla \varphi\|_{L^2(\Omega)}^2 &\leq \|\Delta \varphi\|_{L^2(\Omega)} \|\varphi\|_{L^2(\Omega)} \leq \frac{1}{2} \varepsilon \|\Delta \varphi\|_{L^2(\Omega)}^2 + \frac{1}{2\varepsilon} \|\varphi\|_{L^2(\Omega)}^2 \\ &\leq \frac{1}{2} \varepsilon \|\Delta \varphi\|_{L^2(\Omega)}^2 + \frac{1}{2\varepsilon} \left[\frac{1}{|\Omega|} \left(\int_{\Omega} u(x) dx \right)^2 + c_P \int_{\Omega} |\nabla u(x)|^2 dx \right]. \end{aligned}$$

In particular for $\varepsilon = c_P$ this results in

$$\|\nabla\varphi\|_{L^2(\Omega)}^2 \leq c_P \|\Delta\varphi\|_{L^2(\Omega)}^2 + \frac{1}{c_P |\Omega|} \left(\int_{\Omega} u(x) dx \right)^2,$$

and hence

$$\begin{aligned} \|\varphi\|_{H_{\Delta}^1(\Omega)}^2 &= \|\nabla\varphi\|_{L^2(\Omega)}^2 + \frac{1}{|\Omega|} \left(\int_{\Omega} \varphi(x) dx \right)^2 + \|\Delta\varphi\|_{L^2(\Omega)}^2 \\ &\leq \left(1 + \frac{1}{c_P} \right) \frac{1}{|\Omega|} \left(\int_{\Omega} \varphi(x) dx \right)^2 + (1 + c_P) \|\Delta\varphi\|_{L^2(\Omega)}^2 \\ &\leq \max \left\{ 1 + c_P, 1 + \frac{1}{c_P} \right\} \left[\frac{1}{|\Omega|} \left(\int_{\Omega} \varphi(x) dx \right)^2 + \|\Delta\varphi\|_{L^2(\Omega)}^2 \right] \end{aligned}$$

follows. ■

For $(p, \varphi) \in X \times Y$ we have

$$\begin{aligned} a(p, \varphi) &= \int_{\Omega} p[-\Delta\varphi] dx + \frac{1}{|\Omega|} \int_{\Omega} p dx \int_{\Omega} \varphi dx \\ &\leq \|p\|_{L^2(\Omega)} \|\Delta\varphi\|_{L^2(\Omega)} + \frac{1}{|\Omega|} \int_{\Omega} p dx \int_{\Omega} \varphi dx \\ &\leq \left(\|p\|_{L^2(\Omega)}^2 + \frac{1}{|\Omega|} \left(\int_{\Omega} p dx \right)^2 \right)^{1/2} \left(\|\Delta\varphi\|_{L^2(\Omega)}^2 + \frac{1}{|\Omega|} \left(\int_{\Omega} \varphi dx \right)^2 \right)^{1/2} \\ &= \|p\|_{L^2(\Omega)} \|\varphi\|_Y. \end{aligned} \tag{2.6}$$

Now we are in the position to state unique solvability of the variational problem (2.3).

Theorem 2.2 *Let $(\mathbf{u}, p) \in \mathbf{H}_0^1(\Omega) \times L_0^2(\Omega)$ be the unique solution of the Dirichlet problem for the Stokes system (1.1). Then the pressure $p \in L^2(\Omega)$ is given as the unique solution of the extended variational formulation (2.3), which satisfies the scaling condition (1.3), i.e., $p \in L_0^2(\Omega)$.*

Proof. For $p \in L^2(\Omega)$ we consider the splitting

$$p(x) = p_0(x) + \varrho, \quad \varrho = \frac{1}{|\Omega|} \int_{\Omega} p(x) dx, \quad \int_{\Omega} p_0(x) dx = 0,$$

where we have

$$\|p\|_{L^2(\Omega)}^2 = \int_{\Omega} [p(x)]^2 dx = \int_{\Omega} [p_0(x) + \varrho]^2 dx = \int_{\Omega} [p_0(x)]^2 dx + 2\varrho \int_{\Omega} p_0(x) dx + |\Omega| \varrho^2,$$

i.e.,

$$\|p\|_{L^2(\Omega)}^2 = \|p_0\|_{L^2(\Omega)}^2 + \frac{1}{|\Omega|} \left(\int_{\Omega} p(x) dx \right)^2.$$

Let $\varphi \in H^1(\Omega)$ be the unique weak solution of the Neumann boundary value problem

$$-\Delta\varphi = p_0 \quad \text{in } \Omega, \quad \frac{\partial}{\partial n_x}\varphi = 0 \quad \text{on } \Gamma, \quad \int_{\Omega} \varphi \, dx = \int_{\Omega} p(x) \, dx.$$

Then,

$$\begin{aligned} a(p, \varphi) &= \int_{\Omega} p(x) [-\Delta\varphi(x)] \, dx + \frac{1}{|\Omega|} \int_{\Omega} p(x) \, dx \int_{\Omega} \varphi(x) \, dx \\ &= \int_{\Omega} [p_0(x) + \varrho] p_0(x) \, dx + \frac{1}{|\Omega|} \left(\int_{\Omega} p(x) \, dx \right)^2 \\ &= \int_{\Omega} [p_0(x)]^2 \, dx + \frac{1}{|\Omega|} \left(\int_{\Omega} p(x) \, dx \right)^2 = \|p\|_{L^2(\Omega)}^2 \\ &= \int_{\Omega} [-\Delta\varphi(x)]^2 \, dx + \frac{1}{|\Omega|} \left(\int_{\Omega} \varphi(x) \, dx \right)^2 = \|\varphi\|_Y^2 \end{aligned}$$

implies

$$a(p, \varphi) = \|p\|_{L^2(\Omega)} \|\varphi\|_Y,$$

and therefore the inf-sup condition

$$\|p\|_{L^2(\Omega)} \leq \sup_{0 \neq \varphi \in Y} \frac{a(p, \varphi)}{\|\varphi\|_Y} \quad \text{for all } p \in L^2(\Omega) \quad (2.7)$$

follows. On the other hand, for $0 \neq \varphi \in Y \subset H_{\Delta}^1(\Omega)$ we first compute

$$\alpha = \frac{1}{|\Omega|} \int_{\Omega} \varphi(x) \, dx,$$

then define $p = -\Delta\varphi + \alpha \in L^2(\Omega)$. For this particular choice we obtain

$$\begin{aligned} a(p, \varphi) &= \int_{\Omega} p(x) [-\Delta\varphi(x)] \, dx + \frac{1}{|\Omega|} \int_{\Omega} p(x) \, dx \int_{\Omega} \varphi(x) \, dx \\ &= \int_{\Omega} [-\Delta\varphi(x) + \alpha] [-\Delta\varphi(x)] \, dx + \frac{1}{|\Omega|} \int_{\Omega} [-\Delta\varphi(x) + \alpha] \, dx \int_{\Omega} \varphi(x) \, dx \\ &= \int_{\Omega} [\Delta\varphi(x)]^2 \, dx + \frac{1}{|\Omega|} \left(\int_{\Omega} \varphi(x) \, dx \right)^2 \\ &= \|\varphi\|_Y^2 > 0, \end{aligned}$$

where we have used

$$\int_{\Omega} [-\Delta\varphi(x)] \, dx = - \int_{\Gamma} \frac{\partial}{\partial n_x} \varphi(x) \, ds_x = 0 \quad \text{for } \varphi \in Y.$$

Hence we have that all assumptions of the Babuška–Brezzi theorem are satisfied, see e.g., [3], and therefore unique solvability of (2.3) follows. In particular for $\varphi \equiv 1$ we finally conclude the scaling condition (1.3). \blacksquare

3 Conforming finite element methods

Let

$$X_h = \text{span}\{\psi_k\}_{k=1}^N \subset X = L^2(\Omega)$$

be the space of piecewise constant basis functions ψ_k defined with respect to some admissible decomposition of Ω into finite elements τ_k of local mesh size h_k , and with global mesh size $h = \max_{k=1, \dots, N} h_k$. For simplicity we assume that the mesh is globally quasi-uniform, that is, $h_k \sim h$ for all $k = 1, \dots, N$. Then the finite element variational formulation of (2.3) is to find $p_h \in X_h$ such that

$$\int_{\Omega} p_h [-\Delta \varphi_h] dx + \frac{1}{|\Omega|} \int_{\Omega} p_h dx \int_{\Omega} \varphi_h dx = \int_{\Omega} \tilde{\mathbf{f}} \cdot \nabla \varphi_h dx \quad (3.1)$$

is satisfied for all $\varphi_h \in Y_h$, where the finite element space $Y_h \subset Y$ remains to be specified. At this time we assume $\dim Y_h = \dim X_h$ and the discrete inf-sup or Babuška–Brezzi–Ladyshenskaya condition

$$c_S \|p_h\|_{L^2(\Omega)} \leq \sup_{0 \neq \varphi_h \in Y_h} \frac{a(p_h, \varphi_h)}{\|\varphi_h\|_Y} \quad \text{for all } p_h \in X_h. \quad (3.2)$$

Using standard arguments, see, e.g., [3], we conclude unique solvability of the Galerkin–Petrov scheme (3.1), as well as Cea’s lemma

$$\|p - p_h\|_{L^2(\Omega)} \leq c \inf_{q_h \in X_h} \|p - q_h\|_{L^2(\Omega)}, \quad (3.3)$$

and hence the a priori error estimate

$$\|p - p_h\|_{L^2(\Omega)} \leq c h^s |p|_{H^s(\Omega)} \quad (3.4)$$

when assuming $p \in H^s(\Omega)$ for some $s \in [0, 1]$. In particular for $p \in H^1(\Omega)$ we therefore obtain linear convergence for a piecewise constant approximation p_h .

It remains to define a suitable test space $Y_h = \text{span}\{\varphi_k\}_{k=1}^N \subset Y$ such that the discrete stability condition (3.2) is satisfied. For a given $\varphi_h \in Y_h$ we define $\bar{p}_h = Q_h[-\Delta \varphi_h] \in X_h$ as the piecewise constant L^2 projection satisfying

$$\langle \bar{p}_h, q_h \rangle_{L^2(\Omega)} = \langle -\Delta \varphi_h, q_h \rangle_{L^2(\Omega)} \quad \text{for all } q_h \in X_h. \quad (3.5)$$

In particular for $q_h \equiv 1 \in X_h$, this gives

$$\int_{\Omega} \bar{p}_h(x) dx = \int_{\Omega} [-\Delta \varphi_h(x)] dx = - \int_{\Gamma} \frac{\partial}{\partial n_x} \varphi_h(x) ds_x = 0.$$

From (3.5) we immediately conclude the stability estimate

$$\|\bar{p}_h\|_{L^2(\Omega)} \leq \|\Delta \varphi_h\|_{L^2(\Omega)},$$

which holds for any choice of the finite element test space Y_h . We now assume that Y_h is chosen in such a way that also the reverse inequality

$$\|\bar{p}_h\|_{L^2(\Omega)} \geq c_{Y_h} \|\Delta\varphi_h\|_{L^2(\Omega)} \quad (3.6)$$

is satisfied for a positive constant $c_{Y_h} \leq 1$. Possible choices will be discussed at the end of this section.

We now define

$$p_h(x) = \bar{p}_h(x) + \alpha \in X_h, \quad \alpha = \frac{1}{|\Omega|} \int_{\Omega} \varphi_h(x) dx,$$

which also implies

$$\alpha = \frac{1}{|\Omega|} \int_{\Omega} p_h(x) dx, \quad \int_{\Omega} p_h(x) dx = \int_{\Omega} \varphi_h(x) dx.$$

With this we compute, using (3.6),

$$\begin{aligned} a(p_h, \varphi_h) &= \int_{\Omega} p_h(x) [-\Delta\varphi_h(x)] dx + \frac{1}{|\Omega|} \int_{\Omega} p_h(x) dx \int_{\Omega} \varphi_h(x) dx \\ &= \int_{\Omega} \bar{p}_h(x) [-\Delta\varphi_h(x)] dx + \frac{1}{|\Omega|} \int_{\Omega} p_h(x) dx \int_{\Omega} \varphi_h(x) dx \\ &= \int_{\Omega} [\bar{p}_h(x)]^2 dx + \frac{1}{|\Omega|} \left(\int_{\Omega} p_h(x) dx \right)^2 \\ &= \left[\|\bar{p}_h\|_{L^2(\Omega)}^2 + \frac{1}{|\Omega|} \left(\int_{\Omega} p_h(x) dx \right)^2 \right]^{1/2} \left[\|\bar{p}_h\|_{L^2(\Omega)}^2 + \frac{1}{|\Omega|} \left(\int_{\Omega} p_h(x) dx \right)^2 \right]^{1/2} \\ &\geq c_{Y_h} \left[\|\Delta\varphi_h\|_{L^2(\Omega)}^2 + \frac{1}{|\Omega|} \left(\int_{\Omega} \varphi_h(x) dx \right)^2 \right]^{1/2} \left[\|\bar{p}_h\|_{L^2(\Omega)}^2 + \frac{1}{|\Omega|} \left(\int_{\Omega} p_h(x) dx \right)^2 \right]^{1/2} \\ &= c_{Y_h} \|\varphi_h\|_Y \|p_h\|_{L^2(\Omega)}, \end{aligned}$$

which implies the stability condition

$$c_{Y_h} \|\varphi_h\|_Y \leq \sup_{0 \neq q_h \in X_h} \frac{a(q_h, \varphi_h)}{\|\varphi_h\|_Y} \quad \text{for all } \varphi_h \in Y_h. \quad (3.7)$$

Corollary 3.1 *For $\varphi \in Y$ we can define $\Pi_h\varphi \in Y_h$ as the unique solution of the variational problem*

$$a(q_h, \Pi_h\varphi) = a(q_h, \varphi) \quad \text{for all } q_h \in X_h, \quad (3.8)$$

where unique solvability follows from $\dim X_h = \dim Y_h$ and (3.7). The latter also implies, together with (2.6),

$$c_{Y_h} \|\Pi_h\varphi\|_Y \leq \sup_{0 \neq q_h \in X_h} \frac{a(q_h, \Pi_h\varphi)}{\|q_h\|_{L^2(\Omega)}} = \sup_{0 \neq q_h \in X_h} \frac{a(q_h, \varphi)}{\|q_h\|_{L^2(\Omega)}} \leq \|\varphi\|_Y. \quad (3.9)$$

Now we can prove the discrete stability condition (3.2) when applying the criteria of Fortin [5].

Lemma 3.2 *Let assumption (3.6) be satisfied. Then, there holds the discrete stability condition (3.2) with $c_S = c_{Y_h}$.*

Proof. From the continuous stability condition (2.7), and using (3.8) and (3.9) we conclude

$$\begin{aligned} \|p_h\|_{L^2(\Omega)} &= \sup_{0 \neq \varphi \in Y} \frac{a(p_h, \varphi)}{\|\varphi\|_Y} = \sup_{0 \neq \varphi \in Y} \frac{a(p_h, \Pi_h \varphi)}{\|\varphi\|_Y} \\ &\leq \frac{1}{c_{Y_h}} \sup_{0 \neq \varphi \in Y} \frac{a(p_h, \Pi_h \varphi)}{\|\Pi_h \varphi\|_Y} \leq \frac{1}{c_{Y_h}} \sup_{0 \neq \varphi_h \in Y} \frac{a(p_h, \varphi_h)}{\|\varphi_h\|_Y}. \end{aligned}$$

■

It remains to define the finite element test space $Y_h \subset Y$ such that (3.6) is satisfied with a positive constant c_{Y_h} independent of the discretization parameter h .

3.1 Tensor–product meshes

Since X_h is defined as the space of piecewise constant basis functions we find

$$\bar{p}_k = \bar{p}_h(x) = \frac{1}{|\tau_k|} \int_{\tau_k} [-\Delta \varphi_h(x)] dx \quad \text{for } x \in \tau_k, \quad k = 1, \dots, N.$$

We first consider the one–dimensional case where the computational domain $\Omega = (0, 1)$ is decomposed into N finite elements $\tau_k = (x_{k-1}, x_k)$ of mesh size $h = 1/N$, i.e., $x_k = kh$ for $k = 0, 1, \dots, N$. For a finite element $\tau_k = (x_{k-1}, x_k)$, $k = 1, \dots, N$, the piecewise constant basis function ψ_k is defined as

$$\psi_k(x) = \begin{cases} 1 & \text{for } x \in (x_{k-1}, x_k), \\ 0 & \text{else.} \end{cases}$$

For the definition of a conforming test space $Y_h \subset Y$ we use piecewise quadratic B–splines, i.e., for $k = 2, \dots, N-1$,

$$\varphi_k(x) = \begin{cases} \frac{1}{2} \frac{1}{h^2} (x - x_{k-2})^2 & \text{for } x \in [x_{k-2}, x_{k-1}], \\ \frac{1}{4} \frac{1}{h^2} [3h^2 - (2x - x_{k-1} - x_k)^2] & \text{for } x \in [x_{k-1}, x_k], \\ \frac{1}{2} \frac{1}{h^2} (x - x_{k+1})^2 & \text{for } x \in [x_k, x_{k+1}], \\ 0 & \text{else,} \end{cases} \quad (3.10)$$

while for $k = 1$ and $k = N$ we use the modified splines

$$\varphi_1(x) = \begin{cases} 1 - \frac{1}{2} \frac{1}{h^2} (x - x_0)^2 & \text{for } x \in [x_0, x_1], \\ \frac{1}{2} \frac{1}{h^2} (x - x_2)^2 & \text{for } x \in [x_1, x_2], \\ 0 & \text{else,} \end{cases} \quad (3.11)$$

and

$$\varphi_N(x) = \begin{cases} \frac{1}{2} \frac{1}{h^2} (x - x_{N-2})^2 & \text{for } x \in [x_{N-2}, x_{N-1}], \\ 1 - \frac{1}{2} \frac{1}{h^2} (x - x_N)^2 & \text{for } x \in [x_{N-1}, x_N], \\ 0 & \text{else,} \end{cases} \quad (3.12)$$

to ensure conformity $Y_h \subset Y$ (see Figure 1). For a given $\varphi_h \in Y_h$ we then conclude $\bar{p}_h = -\varphi_h'' \in X_h$, and hence (3.6) follows with $c_{Y_h} = 1$.

In the multi-dimensional cases ($n = 2$ and $n = 3$), we can define Y_h as the tensor product of the one-dimensional test space. But in this case it follows that $-\Delta\varphi_h \notin X_h$ is not piecewise constant, i.e., we need to use the L^2 projection $\bar{p}_h = Q_h[-\Delta\varphi_h] \in X_h$, see (3.5).

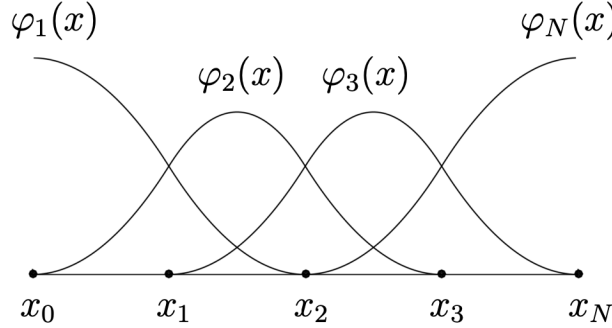


Figure 1: Illustration of the smooth, piecewise quadratic functions used as basis for the one-dimensional test space.

Example 3.1 For a given mesh size h we consider the computational domain $\Omega = (0, 2h)^2$ which is decomposed into 4 finite elements τ_k . When using the one-dimensional basis functions

$$\varphi_1(x) = \begin{cases} 1 - \frac{1}{2} \frac{x^2}{h^2} & \text{for } x \in (0, h), \\ \frac{1}{2} \frac{1}{h^2} (x - 2h)^2 & \text{for } x \in (h, 2h), \end{cases}$$

and

$$\varphi_2(x) = \begin{cases} \frac{1}{2} \frac{x^2}{h^2} & \text{for } x \in (0, h), \\ 1 - \frac{1}{2} \frac{1}{h^2} (x - 2h)^2 & \text{for } x \in (h, 2h), \end{cases}$$

we can write $\varphi_h \in Y_h$ as

$$\varphi_h(x) = a_{11}\varphi_1(x_1)\varphi_1(x_2) + a_{21}\varphi_2(x_1)\varphi_1(x_2) + a_{12}\varphi_1(x_1)\varphi_2(x_2) + a_{22}a_{11}\varphi_2(x_1)\varphi_2(x_2),$$

for which we compute

$$\|\Delta\varphi_h\|_{L^2(\Omega)}^2 = \frac{1}{45} \frac{1}{h^2} \left(\begin{pmatrix} 178 & -88 & -88 & -2 \\ -88 & 178 & -2 & -88 \\ -88 & -2 & 178 & -88 \\ -2 & -88 & -88 & 178 \end{pmatrix} \begin{pmatrix} a_{11} \\ a_{21} \\ a_{12} \\ a_{22} \end{pmatrix}, \begin{pmatrix} a_{11} \\ a_{21} \\ a_{12} \\ a_{22} \end{pmatrix} \right).$$

For the piecewise constant L^2 projection $\bar{p}_h = Q_h[-\Delta\varphi_h] \in X_h$ as defined in (3.5) we obtain

$$\|\bar{p}_h\|_{L^2(\Omega)}^2 = \frac{1}{9} \frac{1}{h^2} \left(\begin{pmatrix} 34 & -16 & -16 & -2 \\ -16 & 34 & -2 & -16 \\ -16 & -2 & 34 & -16 \\ -2 & -16 & -16 & 34 \end{pmatrix} \begin{pmatrix} a_{11} \\ a_{21} \\ a_{12} \\ a_{22} \end{pmatrix}, \begin{pmatrix} a_{11} \\ a_{21} \\ a_{12} \\ a_{22} \end{pmatrix} \right).$$

It is easy to check that the eigenvectors of both matrices coincide, i.e.,

$$\underline{v}^1 = \begin{pmatrix} 1 \\ 1 \\ 1 \\ 1 \end{pmatrix}, \quad \underline{v}^2 = \begin{pmatrix} 1 \\ -1 \\ -1 \\ 1 \end{pmatrix}, \quad \underline{v}^3 = \begin{pmatrix} -1 \\ 0 \\ 0 \\ 1 \end{pmatrix}, \quad \underline{v}^4 = \begin{pmatrix} 0 \\ -1 \\ 1 \\ 0 \end{pmatrix},$$

and for all $\underline{a} \in \mathbb{R}^4$ we can write

$$\underline{a} = \sum_{k=1}^4 \alpha_k \underline{v}^k.$$

With this we compute

$$\|\Delta\varphi_h\|^2 = \frac{1}{45} \frac{1}{h^2} [1408\alpha_2^2 + 360\alpha_3^2 + 360\alpha_4^2]$$

as well as

$$\|\bar{p}_h\|_{L^2(\Omega)}^2 = \frac{1}{9} \frac{1}{h^2} [256\alpha_2^2 + 72\alpha_3^2 + 72\alpha_4^2].$$

Hence we conclude

$$\|\bar{p}_h\|_{L^2(\Omega)}^2 \geq \frac{10}{11} \|\Delta\varphi_h\|_{L^2(\Omega)}^2,$$

which is (3.6) with $c_{Y_h} = 10/11$.

While the approach as given in the previous example can be generalized to any tensor product decomposition of Ω , a rigorous proof of (3.6) remains open. However, the numerical results as given in Section 4 confirm that (3.6) is satisfied also in more general situations.

3.2 Simplicial meshes

As we have just seen, when considering tensor-product spaces we have $\Delta\varphi_h \notin X_h$, which requires showing the reverse inequality (3.6). Moreover, tensor-product meshes impose an obviously strong restriction on the geometries that can be discretized. Also notice that the tensor products of one-dimensional H^2 functions are also in $H^2(\Omega)$, which is in some sense more than we need for stability, since $H^2(\Omega) \subseteq H^1_\Delta(\Omega)$. In this context, we can alternatively construct an appropriate test space by taking functions $\varphi_h \in H^1_\Delta(\Omega)$ so that $\nabla\varphi_h = \boldsymbol{\psi}_h \in \text{RT}_0$ – the lowest-order Raviart–Thomas space. On simplicial meshes (triangles for $n = 2$, tetrahedra for $n = 3$), this space contains piecewise linear, vector-valued functions $\boldsymbol{\psi}_h \in H(\text{div}, \Omega)$. Then, by picking only the basis functions satisfying the boundary condition $\boldsymbol{\psi}_h \cdot \mathbf{n}_x = 0$ on $\partial\Omega$, we will have

$$\Delta\varphi_h = \text{div } \boldsymbol{\psi}_h \in X_h \subset L^2(\Omega),$$

so that stability follows immediately from Lemma 3.2 with $c_{Y_h} = 1$. Note that, since the degrees of freedom of the Raviart–Thomas element are the normal components $\boldsymbol{\psi}_h \cdot \mathbf{n}_x$ on the element edges ($n = 2$) or faces ($n = 3$), it is straightforward to select only those with zero value on $\partial\Omega$. Formally, for each element τ_k , we define the actual scalar test function $\varphi_k \in Y_h \subset Y$ as the unique solution of the Neumann boundary value problem

$$-\Delta\varphi_k = -\text{div } \boldsymbol{\psi}_k \quad \text{in } \Omega, \quad \frac{\partial}{\partial n_x} \varphi_k = 0 \quad \text{on } \Gamma, \quad \int_\Omega \varphi_k \, dx = \alpha_k > 0, \quad (3.13)$$

which gives us

$$\int_\Omega p_h [-\text{div } \boldsymbol{\psi}_k] \, dx + \frac{\alpha_k}{|\Omega|} \int_\Omega p_h \, dx = \int_\Omega \tilde{\mathbf{f}} \cdot \boldsymbol{\psi}_k \, dx.$$

Notice that we can work directly with the Raviart–Thomas functions $\boldsymbol{\psi}_k$ without having to actually solve (3.13) for φ_k , which is thus implicitly defined. The scaling factor α_k can be chosen either mesh dependent, or simply equal to 1, for example. However, since these test functions do not necessarily form a partition of unity, the scaling $p_h \in L^2_0(\Omega)$ is no longer exactly satisfied. This does not matter in practice, since one can solve for p_h and then simply compute

$$\tilde{p}_h = p_h - \frac{1}{|\Omega|} \int_\Omega p_h \, dx,$$

which will then have zero mean, by construction.

For an element τ_k , the support of $\boldsymbol{\psi}_k$ will cover no more than $n + 1$ elements: τ_k itself and all adjacent elements with a common face ($n = 3$) or edge ($n = 2$). We then select $\boldsymbol{\psi}_k \in \text{RT}_0$ such that $\boldsymbol{\psi}_k \cdot \mathbf{n}_x = 1$ on $\partial\tau_k \setminus \Gamma$, $\boldsymbol{\psi}_k \cdot \mathbf{n}_x = -1$ on the common faces ($n = 3$) or edges ($n = 2$) of neighboring elements, and $\boldsymbol{\psi}_k \cdot \mathbf{n}_x = 0$ elsewhere. Figure 2 illustrates the setup in two dimensions, and details on the properties and the implementation of Raviart–Thomas functions can be found in [1].

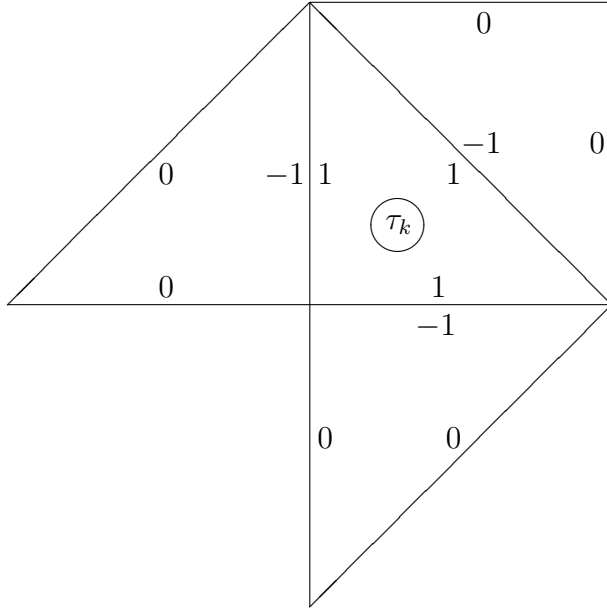


Figure 2: Support of the vector-valued test function $\boldsymbol{\psi}_k \in \text{RT}_0$ and its normal values $\boldsymbol{\psi}_k \cdot \boldsymbol{n}_x$, for an internal element τ_k in two dimensions. The negative values in adjacent elements account for the change in the local definition (direction) of \boldsymbol{n}_x .

4 Numerical results

This section presents some numerical results supporting the a priori estimates. In a square channel $\Omega = (0, 1)^2$, consider the (Navier-)Stokes solution given by

$$\mathbf{u}(x, y) = \begin{pmatrix} y - y^2 \\ 0 \end{pmatrix}, \quad p(x, y) = 1 - 2x,$$

for which we compute the right-hand side vector $\tilde{\mathbf{f}} = (-2, 0)^\top$. We consider three mesh families: simplicial with uniform (red) refinement, tensor-product with uniform refinement, and tensor-product with geometric refinement. In all cases, the coarsest level is a uniform mesh with four elements of equal size. For the third family, the geometric refinement towards the corners is illustrated in Figure 3. The relative $L^2(\Omega)$ pressure errors obtained through the piecewise constant approximations are shown in Table 1, confirming the linear convergence for all discretizations considered. The optimal convergence obtained for the graded meshes indicates that the discrete inf-sup condition computed in Example 3.1 for a simple mesh could be extended to more general discretizations.

5 Conclusions

In this work, we have presented, analyzed and discretized an ultra-weak variational formulation for the pressure Poisson equation. Differently from common approaches, we do

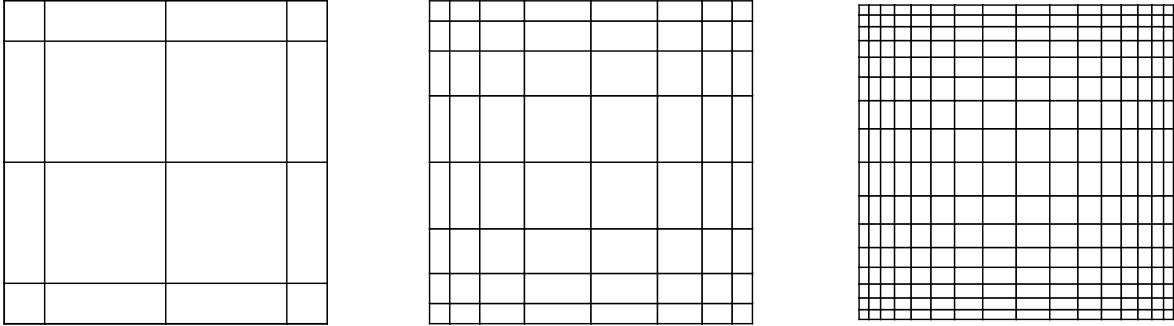


Figure 3: First three levels of geometrical refinement applied to an initial 2×2 mesh.

Table 1: Numerical test case showing the linear convergence of the piecewise constant pressure approximation for different types of discretization.

Number of elements	Simplicial		Tensor-product		Tensor-product, graded	
	L^2 -error	eoc	L^2 -error	eoc	L^2 -error	eoc
4	5.77e-1		7.20e-1		7.20e-1	
16	2.89e-1	1.00	3.54e-1	1.02	3.51e-1	1.03
64	1.44e-1	1.00	1.80e-1	0.97	1.70e-1	1.05
256	7.22e-1	1.00	9.07e-2	0.99	8.30e-2	1.03
1,024	3.61e-1	1.00	4.54e-2	1.00	4.10e-2	1.02
4,096	1.80e-1	1.00	2.27e-2	1.00	2.04e-2	1.01
16,384	9.02e-2	1.00	1.13e-2	1.00	1.02e-2	1.00
32,768	4.51e-2	1.00	5.68e-3	1.00	5.08e-3	1.00

not rely on a discontinuous Galerkin framework, nor do we recast the Poisson problem into a mixed first-order system, but rather consider a scalar Galerkin–Petrov formulation. To that end, we use an additional round of integration by parts to get rid of all derivatives on the trial functions p , which allows us to consider $p \in L^2(\Omega)$ as in the Navier–Stokes system. As a trade-off, we must have H^1 test functions with square-integrable Laplacian, hence the Galerkin–Petrov nature of our framework. When considering these different trial and test spaces, unique solvability of the continuous problem is guaranteed by an inf-sup stability condition. We have then also proved discrete stability and a priori error estimates for a conforming, yet abstract choice of spaces fulfilling certain conditions. When considering piecewise constant trial functions, two realizations of the test space are provided. For tensor-product meshes, modified second-order B-splines can be used as test functions; in that case, the discrete inf-sup condition is proven in one dimension, while an extension to higher dimensions is sketched. For simplicial elements, we can use test functions whose gradients are in the lowest-order Raviart–Thomas space, which allows a simple implementation on unstructured meshes. The numerical experiments in two dimensions indicate that stability and optimal convergence can be attained also for non-uniform, adaptively refined meshes. An open problem is extending the discretization to higher-order trial spaces. In

fact, first numerical experiments combining piecewise (bi-)linear *ansatz* with Hermite or Argyris polynomials as test functions reveal promising results [8]. Ongoing work includes using the ultra-weak PPE to both reconstruct pressure from measured velocities and stabilize lowest-order discretizations of the Stokes system, similarly to what was done in [9] for continuous pressure.

References

- [1] C. Bahriawati, C. Carstensen: Three Matlab implementations of the lowest-order Raviart–Thomas Mfem with a posteriori error control. *Comput. Methods Appl. Math.*, 5(4):333–361, 2005.
- [2] M. Berggren: Approximations of very weak solutions to boundary–value problems. *SIAM J. Numer. Anal.*, 42(2):860–877, 2004.
- [3] A. Ern, J.–L. Guermond: *Theory and Practice of Finite Elements*, volume 159 of *Applied Mathematical Sciences*. Springer, New York, 2004.
- [4] A. Ern, M. Vohralík, M. Zakerzadeh: Guaranteed and robust L^2 -norm a posteriori error estimates for 1D linear advection problems. *ESAIM: Math. Modelling Numer. Anal.*, 55:S447–S474, 2021.
- [5] M. Fortin: An analysis of the convergence of mixed finite element methods. *RAIRO. Analyse numérique*, 11(4):341–354, 1977.
- [6] H. Johnston, J.–G. Liu: Accurate, stable and efficient Navier–Stokes solvers based on explicit treatment of the pressure term. *J. Comput. Phys.*, 199(1):221–259, 2004.
- [7] D. Nolte, J. Urbina, J. Sotelo, L. Sok, C. Montalba, I. Valverde, A. Osses, S. Uribe, C. Bertoglio: Validation of 4D flow based relative pressure maps in aortic flows. *Med. Image Anal.*, 74:102195, 2021.
- [8] D. R. Q. Pacheco: *Stable and stabilised finite element methods for incompressible flows of generalised Newtonian fluids*, volume 42 of *Computation in Engineering and Science (CES)*. Verlag der Technischen Universität Graz, Graz, 2021.
- [9] D. R. Q. Pacheco, R. Schussnig, O. Steinbach, T.–P. Fries: A global residual-based stabilization for equal-order finite element approximations of incompressible flows. *Int. J. Numer. Methods Eng.*, 122(8):2075–2094, 2021.
- [10] D. R. Q. Pacheco, O. Steinbach: A continuous finite element framework for the pressure Poisson equation allowing non-Newtonian and compressible flow behavior. *Int. J. Numer. Meth. Fluids*, 93:1435–1445, 2021.

- [11] R. L. Sani, J. Shen, O. Pironneau, P. M. Gresho: Pressure boundary condition for the time-dependent incompressible Navier–Stokes equations. *Int. J. Numer. Meth. Fluids*, 50(6):673–682, 2006.